Clay minerals and the adsorption of fullerenes: clues from iridium-enriched Cretaceous–Palaeogene Anjar intertrappean beds, Kachchh district, Gujarat, India

Pronoy Roy[1,3], G. Parthasarathy[2] and Bulusu Sreenivas[1,3,*]

[1]CSIR-National Geophysical Research Institute, Hyderabad 500 007, India
[2]School of Natural Sciences and Engineering, National Institute of Advanced Studies, Indian Institute of Science Campus, Bengaluru 560 012, India
[3]Academy of Scientific and Innovative Research, Ghaziabad 201 002, India

Here we present powder X-ray diffraction (XRD) and Fourier transform infrared (FT-IR) spectroscopic data on clay minerals associated with the iridium (Ir)-enriched and fullerene-bearing yellowish-brown clayey layers of the Anjar intertrappean beds, Kachchh district, Gujarat, India. The objective is to understand the role of clay minerals composition in preserving the fullerene molecules and Ir contents in the Anjar intertrappean beds. XRD patterns show the presence of smectite along with palygorskite and sepiolite. FT-IR spectra also confirm the presence of these Mg-rich clay minerals and broadened peaks indicate their nanocrystalline nature. The study shows a correlation between the nature of smectites and the occurrence of fullerenes and iridium.

Keywords: Clay minerals, Cretaceous–Palaeogene boundary, fullerenes, iridium.

THE Cretaceous–Palaeogene (K–Pg boundary) bolide impact hypothesis has been accepted worldwide since the discovery of iridium anomaly in the 1980s (ref. 1). Since then, several K–Pg boundary sequences like Agost (Spain), Caravaca (Spain), Gubio (Italy), Petruccio (Italy) and El Kef (Tunisia) have been recorded as some of the well-preserved worldwide K–Pg sections. The identification of K–Pg sections is primarily based on biozonation with marked changes in the benthic foraminiferal distribution[2]. Several other geochemical markers such as high iridium anomaly, platinum group inter-elemental ratios, the presence of spherules, high-pressure polymorphs of silica, Ni-rich spinel, traces of meteorite, presumably extraterrestrial helium, the occurrence of diamonds[3–9] and the chemical–mineralogical attributes of clay minerals[10]. Fullerenes (C_{60} molecules) were also reported from major K–Pg boundaries[10–13]. A combination of hydrocarbons and fullerenes has also been reported, e.g. from the Woodside Creek and Flaxbourne River sections of New Zealand[12]. The biomarkers, including alkanes, fatty acids and polycyclic aromatic hydrocarbon (PAH) compounds, were reported from the K–Pg sections of Kawaruppu[14,15] and Um-Sohryngkew river, which is a shallow marine section, and Mahadeva–Cherapunji shelf facies successions in Meghalaya, India. Detection of fullerenes requires proper sampling of the K–Pg sections[16,17]. Both impact-related, volcanism-induced and impact-triggered Deccan volcanism activities have been proposed as the causal factors leading to catastrophic mass extinction and environmental changes[18,19].

The Deccan Volcanic Province (DVP), Meghalaya and the Cauvery Basin are the three important sections where the K–Pg boundary is reported from India. The main pulse of Deccan volcanism occurred within 0.8 Ma of the K–Pg transition[19–21]. The Anjar intertrappean section from Gujarat is one of the well-studied sections for recognizing K–Pg successions. The Anjar section preserves three horizons consisting of chocolate-brown clay layers (<1 cm thick, separated from each other by 25–30 cm) showing anomalously high values of iridium, osmium and other siderophile elements along with chalcophiles (Se, Sb, Ag, As and Zn)[22].

Micropalaeontological studies revealed the abundance of theropod eggshell fragments from the beds overlying Ir-enriched layers, followed by the absence of Paleocene taxa[23]. The Indian subcontinent dinosaur extinction occurred after the deposition of Ir-rich sediments. The Deccan volcanic activity started in the Anjar area, within the uppermost Maastrichtian Chron C30N at 66.5–67 Ma, as indicated by the palaeomagnetic and ^{40}Ar–^{39}Ar ages[24]. There was a 1–2 Ma gap during which volcanic activity stagnated, allowing the deposition of lacustrine-like Maastrichtian sediments. The volcanic activity was reactivated after the K–Pg boundary, and three lava flows were found within the C29R. The non-uniform and inhomogeneous Ir-rich layers have more than one level of succession deposited within the C29R (ref. 25), providing evidence of K–Pg impact[24]. This succession shows facies variation both laterally and vertically, consisting of interlayered, peloidal, cherty limestone and shale[26].

Studies related to the high-pressure phase of fullerenes and Ir in the Anjar intertrappean bed revealed the presence

*For correspondence. (e-mail: bsreenivas@ngri.res.in)

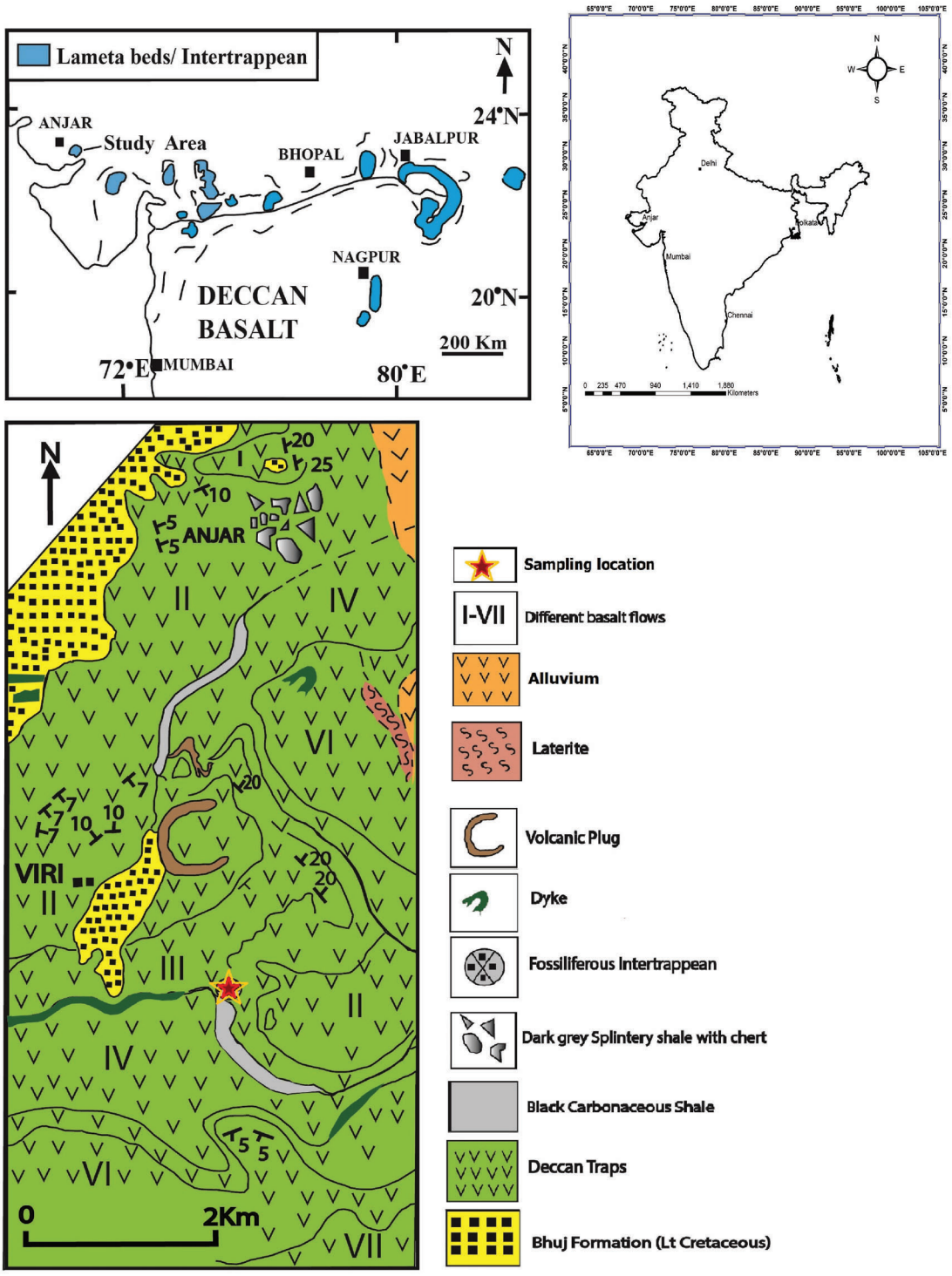

Figure 1. Geological map of the Anjar region, Kachchh district, Gujarat, India showing seven different volcanic flows. (Inset) Map showing the occurrence of various intertrappean beds in the Deccan Volcanic Province.

of C_{60} high-pressure forms of carbon with the help of ^{13}C nuclear magnetic resonance (NMR), ultraviolet (UV)–visible, and Fourier transform infrared (FT-IR) spectroscopy[17,27]. Other studies reported aliphatic compounds in the Anjar intertrappean beds and interpreted them to be formed due to Deccan volcanism[28–30]. The present study discusses the characterization of clay minerals by powder X-ray diffraction (XRD) and FT-IR spectroscopic methods. The results of this study may help improve our understanding of the relationship between clay minerals composition, the Ir content and the high-pressure phase of fullerenes.

Geological setting

The Anjar volcano-sedimentary sequence lies in the western proximity of the DVP, which consists of nine lava flows and four intertrappean beds[31,32]. It was established that the K–Pg boundary occurs at the third intertrappean bed between the third and fourth lava flows[22]. This intertrappean bed is well developed (6 m thick) and consists of cherty limestone, shale and mudstone (Figure 1). There are about three limonitic layers, especially in the lower 1.5 m portion of the intertrappean bed exposed in pit BG-1 (ref. 28). The limonitic layers are enriched in iridium (650–1333 pg/g) and osmium (650–2230 pg/g) in comparison to other horizons[22], while different layers have <100 pg/g of iridium. The geochronological, geochemical and palaeomagnetic studies and palaeontological data suggest that limonitic layer deposition was close to the K–Pg boundary[22,24]. The intertrappean sediment deposition rate was rapid compared to contemporary marine sections; hence, intertrappean beds preserve better time resolution.

Materials and methods

Nine samples from the intertrappean bed were collected from pit BG-1 and analysed using XRD and FT-IR. Figure 1 shows the stratigraphic location of these samples for three Ir-rich layers (BR-1, BR-2, BR-3)[28]. Sample 964 is located just below the Ir-rich brown layer (BR-1). Sample L is the limonitic layer (BR-2) having maximum Ir and Os concentration. Samples J and M represent the third Ir-rich layer (BR-3). Sample M was collected from about 3 m laterally away from sample J.

The XRD patterns were obtained using a Siemens D-5000 powder diffractometer with HOPG graphite monochromator at the CSIR-Indian Institute of Chemical Technology (IICT), Hyderabad. Copper K-α radiation of 0.15406 nm was used in all the diffraction experiments. FT-IR studies on the samples were carried out in ambient conditions using a BIORAD 175C FT-IR spectrometer following the potassium bromide pellet method at CSIR-IICT. Samples were scanned in the frequency range 4000–300 cm^{-1}. Each sample was scanned three times. The typical uncertainty in the wavenumber was ±3 cm^{-1} in the frequency range 2000–4000 cm^{-1}.

Table 1. Clay mineral assemblages in Anjar samples indicated by XRD analysis

Depth (cm)	Sample	Clay mineral assemblage
500	947-B	Smectite, palygorskite (weak), carbonate (dominant)
505	953	Smectite, carbonate
507	964	Palygorskite, smectite (amorphous)
533	L	Smectite, palygorskite, carbonate
565	J	Smectite, sepiolite, palygorskite
565	M	Smectite, palygorskite
575	96/3	Illite, smectite

Results

XRD analysis

The XRD results show that smectite clay mineral is common in all the samples (Table 1; Figure 2). In some samples, the amorphous/nanocrystalline nature of smectites was revealed by the broad nature of the XRD peaks. Palygorskite, Mg-clay mineral [$(Mg,Al)_2Si_4O_{10}(OH)_4(H_2O)$] is significantly present, especially in samples L, J, M, 964, 947B having dominant peak values at 10.2, 8.77, 4.49, 4.27, 3.36 and 2.54 Å. Sepiolite [$(Mg_4Si_6O_{15}(OH)_26H_2O)$], a variety of palygorskite, was also identified with peaks 2.58 and 3.36 Å, and it overlapped with the palygorskite peaks. The 1.87 Å peak is typical of sepiolite minerals. Illite was present in only one sample (96/3; the lowermost sample), showing a dominant illite peak in the XRD analysis.

FT-IR analysis

The FT-IR spectra suggest that palygorskite and sepiolite, along with smectite, are the main clay minerals (Figure 3 and Table 2). The broad hydrous phases observed indicate the presence of different types of hydrous molecules in the structure of smectites and palygorskite with a considerable amount of induced stress and the OH group coordinated with metallic cations. The wavenumber 3615 cm^{-1} is the

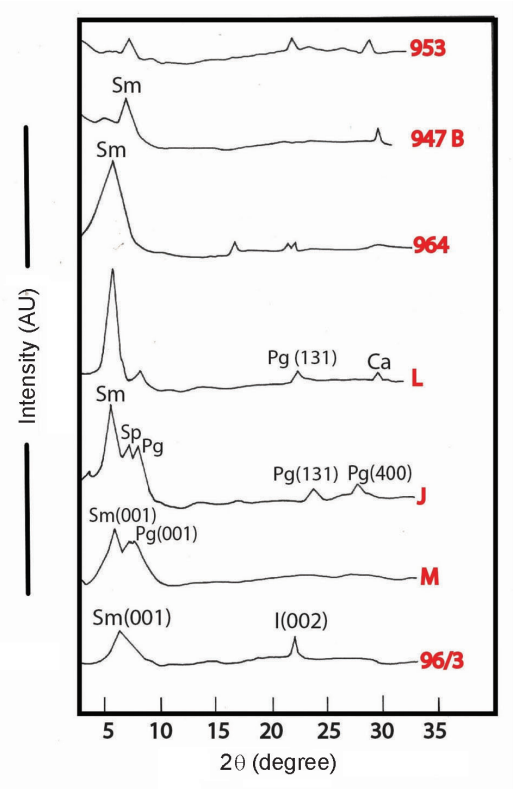

Figure 2. XRD patterns of clay minerals from Anjar samples.

Table 2. FT-IR peaks and assignment of clay minerals in the Anjar samples

Sample (depth, cm)	96/3 (575)	L (533)	964 (507)	953 (505)	Assignment
Characteristic wavenumber (cm)	3620	3625	3622	3615	Palygorskite
	3565	3405	3400	3540	Palygorskite
	3410			3450	
	3248			3410	
	1660	1600	1595	1670	
				1645	
				(Mg-rich Palygorskite)	
	1212	1035	1030	1198	Palygorskite
	1010			1128	
				1090	
				1040	
		912	915	990	Palygorskite
	790	835	840	800	Palygorskite
			798	740	
	697	618	693	645	Palygorskite
	646		620	580	
		523	520	512	
	480	470	468	440	
	(Palygorskite)		345	413	
				375	
				340	

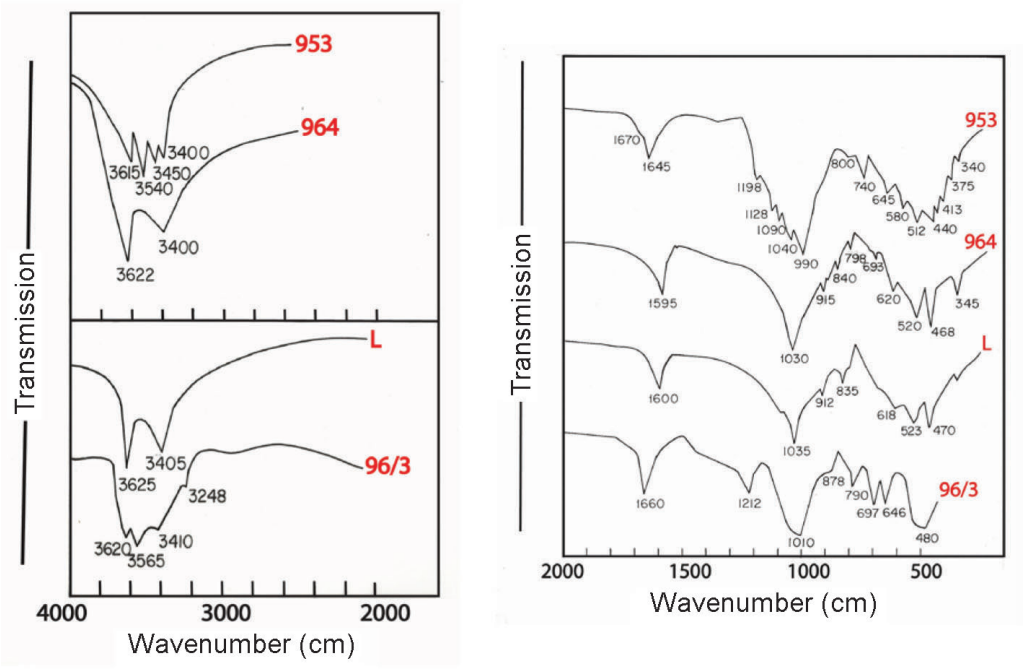

Figure 3. FT-IR spectra of clay minerals.

characteristic peak for palygorskite assigned to the stretching mode of structural hydroxyls bonded to Al cations (Al–OH stretching) in octahedral coordination[33].

Discussion

The XRD and FT-IR results suggest the predominance of sepiolite, palygorskite and smectites. Palygorskite is present mainly in samples J, L, M and 964. Interestingly, all these samples have higher Ir concentrations suggesting a correlation among fullerenes, platinum-group elements and Mg-rich clay minerals like palygorskite and sepiolite. Earlier studies have also reported a relationship between Ir and the Mg-rich clay mineral phases[28–30]. Smectite is a common mineral, and positive excursions in its content in the worldwide K–Pg boundary sections are reported indicating

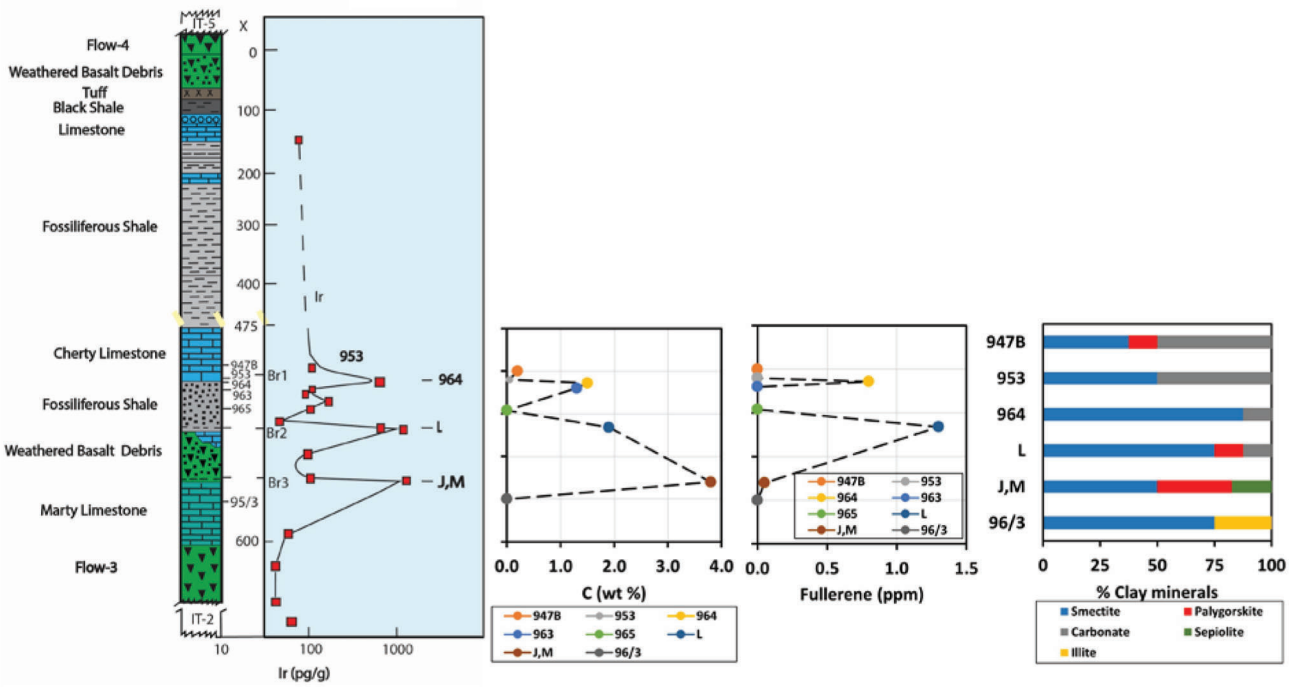

Figure 4. Correlation among iridium, carbon, fullerene and clay mineral assemblage of Anjar samples.

extreme arid environments[34]. The palygorskite and sepiolite clay minerals have been primarily reported from the Anjar and Jhilmili intertrappean beds[30,31]. These Mg-rich clay mineral occurrences are genetically related to hydrothermal alteration of post-eruption of the Deccan basalts[29]. Illite found in the basal section points to the arid environment[35].

The fullerene-related compounds have been reported from the K–Pg boundary[11–13]. Earlier studies on fullerenes in the Anjar Intratrappean beds with the help of NMR, FT-IR, and UV-IR spectroscopy suggested the presence of C_{60} compounds formed due to high pressure[13,17,34]. A correlation was observed between samples with high Ir, Os and fullerene concentrations and those of the palygorskite–smectite–sepiolite assemblage (Figure 4). The absence of fullerenes in sample 953 can be related to the lack of palygorskite and sepiolite clay minerals. The Ir-poor layer shows some complex carbon compounds[17]. Natural palygorskite and vermiculite have a high adsorption capacity of transition metals Cu and Ni (ref. 36). Fullerenes are known to get adsorbed onto ultra-stabilized zeolite Y (USY), especially to the more hydrophobic variety[36], such as a Faujasite molecular sieve with 7.4 Å having three-dimensional pore structure[37]. Fullerence (C_{60}) is a spherical molecule that is highly symmetric and made up of 60 carbon atoms with a diameter of 0.7 nm, and hence fullerences get trapped in faujasite. Apart from transition metals, the acid-treated palygorskite is efficient in adsorbing cationic dyes because of electrostatic effects[38]. Due to its open structure and microfibrous morphology, sepiolite has a high specific surface area (340 $m^2 g^{-1}$) and a large micropore volume (0.44 $m^3 g^{-1}$). The organic molecules can be retained in the structural tunnels formed due to discontinuities in the silicate sheets of sepiolite and at the surface by interacting with silanol groups[39]. Recently, it has been shown that the graphene/sepiolite mixture (2/98, w/w) is effective in adsorbing polycyclic aromatic hydrocarbons[39]. The observed correlation between the abundance of palygorskite–sepiolite and fullerenes in the Anjar section might reveal the adsorption of heavy carbon molecules by these Mg-rich clay minerals (Figure 4).

The Anjar intertrappean beds consist of palygorskite, sepiolite and smectite assemblage, indicating arid environments. Such clay mineral assemblages are typical to the intertrappean sections (e.g. Anjar, Jhilmili, Rajahmundry). Smectite is a characteristic mineral formed in arid environments with poor drainage. Studies based on palynological evidence suggest that these intertrappean beds are deposited in arid environments[30].

In contrast, other K–Pg sections revealed the presence of dominant kaolinite, indicating a humid tropical climate[40,41]. The well-established K–Pg boundary section of the Um-Songhrykew river (Meghalaya), considered one of the complete sections, also has dominant kaolinite minerals, indicating a humid climate[34,42]. The lack of kaolinites in the intertrappean beds is regarded as ‘mock aridity’ caused due to extensive Deccan volcanism[41,42].

The presence of fullerenes also shows a correlation with high Ir-rich layers[17,25]. The correlation among clay minerals (palygorskite–sepiolite–smectite), Ir, C and fullerene indicates that the adsorbing capacity of the microfibrous nature of phyllosilicates has played an important role. The Ir-poor zones did not show the presence of fullerenes, but had

some complex hydrocarbons (PAH)[25]. The presence of high-pressure fullerenes and Ir indicates their impact-related origin and incorporation into the geochemical cycles. The formation of Mg-rich clay minerals in intertrappean strata is linked to the mafic nature of the Deccan basalts. The absence of Ir and fullerenes in many other K–Pg sections may be due to the different adsorbing capacities of clay minerals and the assimilation of impact-related geochemical markers in their local environments.

Conclusion

XRD and FT-IR analysis of the Anjar clay samples indicated the presence of Mg-rich clay minerals such as smectite, palygorskite and sepiolite. The broadening of the FT-IR peaks of these Mg-rich clay minerals may point to their nanocrystalline nature.

The observed correlation among clay minerals assemblage, the concentration of iridium, fullerenes, and carbonaceous matter (C %) suggests the adsorption of fullerenes and chalcophile elements into the structural tunnels of these clay minerals.

The formation of Mg-rich clay minerals is attributed to the alteration of mafic Deccan basalts, and increased concentrations of high-pressure fullerenes and iridium suggest their participation in the geochemical cycles almost coinciding with the K–Pg transition.

1. Alvarez, L. W., Alvarez, W., Asaro, F. and Michel, H. V., Extraterrestrial cause for the Cretaceous–Tertiary extinction. *Science*, 1980, **208**, 1095–1108.
2. Culver, S. J., Benthic foraminifera across the Cretaceous–Tertiary (K–T) boundary: a review. *Mar. Micropaleontol.*, 2003, **47**, 177–226.
3. Kyte, F. T., A meteorite from the Cretaceous–Tertiary boundary. *Nature*, 1998, **396**, 237–239.
4. Shukolyukov, A. and Lugmair, G. W., Isotopic evidence for the Cretaceous–Tertiary impactor and its type. *Science*, 1998, **282**, 927–929.
5. Sutherland, F. L., Volcanism around K/T boundary time – its role in an impact scenario for the K/T extinction events. *Earth Sci. Rev.*, 1994, **36**, 1–26.
6. Smit, J., The global stratigraphy of the Cretaceous–Tertiary boundary impact ejecta. *Annu. Rev. Earth Planet. Sci.*, 1999, **27**, 75–113.
7. Becker, L., Poreda, R. J. and Bunch, T. E., Fullerenes: an extraterrestrial carbon carrier phase for noble gases. *Proc. Natl. Acad. Sci. USA*, 2000, **97**, 2979–2983.
8. Keller, G., Stinnesbeck, W., Adatte, T. and Stueben, D., Multiple impacts across the Cretaceous–Tertiary boundary. *Earth Sci. Rev.*, 2003, **62**, 327–363.
9. Bauluz, B., Peacor, D. R. and Elliott, W. C., Coexisting altered glass and Fe–Ni oxides at the Cretaceous–Tertiary boundary, Stevns Klint (Denmark): direct evidence of meteorite impact. *Earth Planet. Sci. Lett.*, 2000, **182**, 127–136.
10. Keller, G., Adatte, T., Stinnesbeck, W., Stueben, D. and Berner, Z., Age, chemo- and biostratigraphy of Haiti spherule-rich deposits: a multi-event K–T scenario. *Can. J. Earth Sci.*, 2001, **38**, 197–227.
11. Heymann, D., Chibante, L. P. F., Brooks, P. R., Wolbach, W. S. and Smalley, R. E., Fullerenes in the K/T boundary layer. *Science*, 1994, **265**, 645–647.
12. Heymann, D. *et al.*, Fullerenes of possible wildfire origin in Cretaceous–Tertiary boundary sediments. *Geol. Soc. Am. Spec. Pap.*, 1996, **307**, 455–464.
13. Heymann, D., Yancey, T. E., Wolbach, W. S., Thiemens, M. H., Jhonson, E. A., Roach, D. and Moecker, S., Geochemical markers of the Cretaceous–Tertiary boundary event at Brazos River, Texas, USA. *Geochim. Cosmochim. Acta*, 1998, **62**, 173–181.
14. Mita, H. and Shimoyama, A., Characterization of *n*-alkanes, pristane and phytane in the K/T boundary sediments at Kawaruppu, Hokkaido, Japan. *Geochem. J.*, 1999, **33**, 285–294.
15. Shimoyama, A. and Yabuta, H., Mono- and bicyclic alkanes and diamondoid hydrocarbons in the Cretaceous/Tertiary boundary sediments at Kawaruppu, Hokkaido, Japan. *Geochem. J.*, 2002, **36**, 173–189.
16. Buseck, P. R., Geological fullerenes: review and analysis. *Earth Planet. Sci. Lett.*, 2002, **203**, 781–792.
17. Parthasarathy, G., Bhandari, N., Vairamani, M. and Kunwar, A. C., High-pressure phase of natural fullerene C60 in iridium-rich Cretaceous–Tertiary boundary layers of Deccan intertrappean deposits, Anjar, Kutch, India. *Geochim. Cosmochim. Acta*, 2008, **72**, 978–987.
18. Hull, P. M. *et al.*, On impact and volcanism across the Cretaceous–Paleogene boundary. *Science*, 2020, **367**, 266–272.
19. Schoene, B., Eddy, M. P., Samperton, K. M., Keller, C. B., Keller, G., Adatte, T. and Khadri, S. F. R., U–Pb constraints on pulsed eruption of the Deccan traps across the end-cretaceous mass extinction. *Science*, 2019, **363**, 862–866.
20. Schoene, B. *et al.*, U–Pb geochronology of the Deccan Traps and relation to the end-Cretaceous extinction. *Science*, 2015, **347**, 182–184.
21. Renne, P. R., Sprain, C. J., Richards, M. A., Self, S. and Vanderkluysen, L., State shift in Deccan volcanism at the Cretaceous–Paleogene boundary, possibly induced by impact. *Science*, 2015, **350**, 76–78.
22. Bhandari, N. and Shukla, P. N., K/T boundary layer in Deccan intertrappeans at Anjar, Kutch. *Geol. Soc. Am. Spec. Pap.*, 1996, **307**, 417–424.
23. Bajpai, S. and Prasad, G. V. R., Cretaceous age for Ir-rich Deccan intertrappean deposits: palaeontological evidence from Anjar, western India. *J. Geol. Soc. London*, 2000, **107**, 257–260.
24. Courtillot, V. *et al.*, Cosmic markers, $^{40}Ar/^{39}Ar$ dating and paleomagnetism of the KT sections in the Anjar area of the Deccan large igneous province. *Earth Planet. Sci. Lett.*, 2000, **182**, 137–156.
25. Shukla, P. N., Shukla, A. D. and Bhandari, N., Geochemical characterisation of the Cretaceous–Tertiary boundary sediments at Anjar, India. *Palaeobotanist*, 1997, **46**, 127–132.
26. Khadkikar, A. S., Sant, D. A., Gogte, V. and Karanth, R. V., The influence of Deccan volcanism on palaeoclimate during K/T: insights from lacustrine intertrappean deposits, Anjar, western India. *Palaeogeogr. Palaeoclimatol. Palaeoecol.*, 1999, **147**, 141–148.
27. Parthasarathy, G., Bhandari, N., Vairamani, M., Kunwar, A. C. and Narasaiah, B., Natural fullerenes from the Cretaceous–Tertiary boundary layer at Anjar, Kutch, India. *Geol. Soc. Am. Spec. Pap.*, 2002, **356**, 345–350.
28. Shrivastava, J. P., Salil, M. S. and Pattanayak, S. K., Clay mineralogy of Ir-bearing intertrappean, Kutch, Gujrat, India: Inference on paleoenvironment. *J. Geol. Soc. India*, 2000, **55**, 197–206.
29. Shrivastava, J. P. and Ahmad, M., Compositional studies on organic matter from iridium-enriched Anjar intertrappean sediments: Deccan volcanism and palaeoenvironmental implications during the Cretaceous/Tertiary boundary. *J. Iber. Geol.*, 2005, **31**, 167–177.
30. Shrivastava, J. P. and Ahmad, M., Trace element compositions of iridium-enriched illite–smectite assemblages from a K/Pg boundary section in the Anjar area of the Deccan volcanic province: palaeoenvironmental implications. *Cretac. Res.*, 2008, **29**, 592–602.
31. Bhandari, N., Shukla, P. N., Ghevaria, Z. G. and Sundaram, S. M., Impact did not trigger Deccan volcanism: evidence from Anjar K/T

boundary intertrappean sediments. *Geophys. Res. Lett*., 1995, **22,** 433–443.
32. Ghevariya, Z. G., Inter-trappean dinosaurian fossils from Anjar area, Kachchh district, Gujarat. *Curr. Sci*., 1988, **57**, 248–251.
33. Cai, Y., Xue, J. and Polya, D. A., A Fourier transform infrared spectroscopic study of Mg-rich, Mg-poor and acid leached palygorskites. *Spectrochim. Acta, Part A*, 2007, **66**, 282–288.
34. Pal, S., Shrivastava, J. P. and Mukhopadhyay, S. K., Mineral chemistry of clays associated with the late Cretaceous–early Palaeogene succession of the Um Sohryngkew river section of Meghalaya: palaeoenvironmental inferences and K/Pg transition. *J. Geol. Soc. India*, 2015, **86**, 631–647.
35. Samant, B. and Mohabey, D. M., Deccan volcanic eruptions and their impact on flora: palynological evidence. *Geol. Soc. Am. Spec. Pap.*, 2014, **505**, 505–508.
36. Ellison, E. H., Adsorption and photophysics of fullerene C60 at liquid–zeolite particle interfaces: unusually high affinity for hydrophobic, ultrastabilized zeolite Y. *J. Phys. Chem. B*, 2006, **110**, 11406–11414.
37. Bhatia, S., *Zeolite Catalysis: Principles and Applications*, CRC Press, Florida, USA, 1990, pp. 7–12.
38. Yang, R., Li, D., Li, A. and Yang, H., Adsorption properties and mechanisms of palygorskite for removal of various ionic dyes from water. *Appl. Clay Sci*., 2018, **151**, 20–28.
39. Mateos, R., Vera-López, S., Saz, M., Díez-Pascual, A. M. and Paz San Andrés, M., Graphene/sepiolite mixtures as dispersive solid phase extraction sorbents for polycylic aromatic hydrocrabons in wastewater using surfactant aqueous solutions for desorption. *J. Chromatogr. A*, 2019, **1596**, 30–40.
40. Gertsch, B., Keller, G., Adatte, T., Garg, R., Prasad, V., Berner, Z. and Fleitmann, D., Environmental effects of Deccan volcanism across the Cretaceous–Tertiary transition in Meghalaya, India. *Earth Planet. Sci. Lett.*, 2011, **310**, 272–285.
41. Pal, S., Srivastava, S. and Shrivastava, J. P., Environmental effects of Deccan volcanism on biotic transformations and attendant Cretaceous/Paleogene boundary mass extinction in the Indian subcontinent: organo-molecular evidence. *Geol. Soc. Am. Spec. Pap*., 2020, **544**, 165–197; https://doi.org/10.1130/2019.2544(07)
42. Harris, J. and Van Couvering, J., Mock aridity and the paleoecology of volcanically influenced ecosystems. *Geology*, 1995, **23**, 593–596.

ACKNOWLEDGEMENTS. We dedicate this article to the 80th birthday of Prof. R. Srinivasan, expressing our gratitude towards his mentoring in the field of geological sciences. We thank the Directors of CSIR-National Geophysical Research Institute and CSIR-Indian Institute of Chemical Technology for their encouragement and support. We also thank Prof. N. Bhandari (Physical Research Laboratory, Ahmedabad) for providing samples of the Anjar section. G.P. thanks Indian National Science Academy (INSA) and National Institute of Advanced Studies for funds through the INSA Senior Scientist Fellowship. P.R. and B.S. acknowledge AcSIR for the support. This work is part of the CSIR-NGRI in-house project MLP-6406-28.

Received 25 July 2022; revised accepted 28 September 2022

doi: 10.18520/cs/v124/i1/87-93